Supplementary Information

One-Dimensional High-Density Monodispersed Fe_3O_4 Nanoparticles@Carbon Nanotubes Hybrid Nanocomposite for Highly Lithium and Sodium Storage

Xiujuan Wang[a], Xiaojie Liu[a], Gang Wang[b], Yuan Xia [a], Hui Wang[a*]

[a]*Key Laboratory of Synthetic and Natural Functional Molecule Chemistry (Ministry of Education), College of Chemistry & Materials Science, Northwest University, Xi'an 710069, PR China*

[b]*National Key Laboratory of Photoelectric Technology and Functional Materials (Culture Base), National Photoelectric Technology and Functional Materials & Application International Cooperation Base, Institute of Photonics & Photon-Technology, Northwest University, Xi'an 710069, PR China*

[*]Corresponding author:

Tel.: +86 029 88363115

Fax: +86 29 88302571

E-mail address: huiwang@nwu.edu.cn (H. Wang).

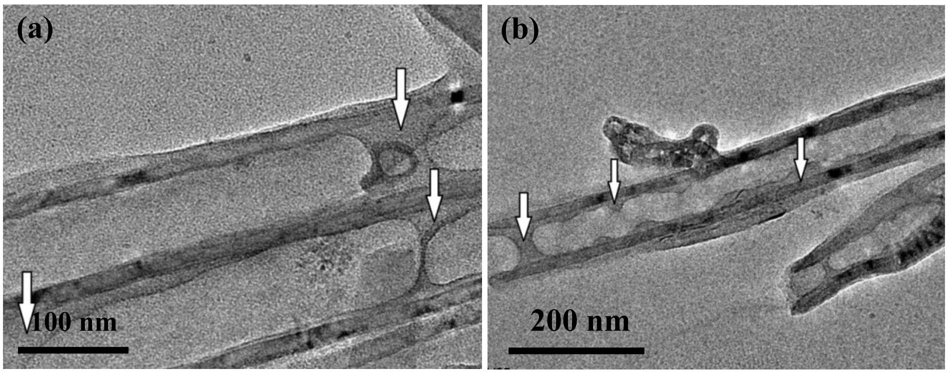

Fig. S1 The TEM images after iron stearate octadecene solution filling CNTs cavity (a) and before being heated up for decomposition (b).

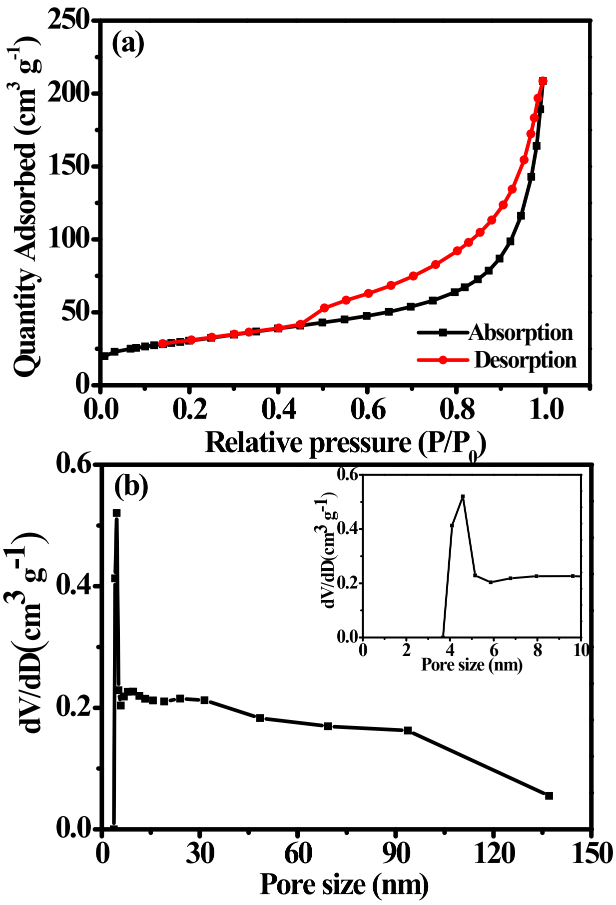

Fig. S2 (a) N_2 sorption isotherms and (b) pore size distribution of CNTs

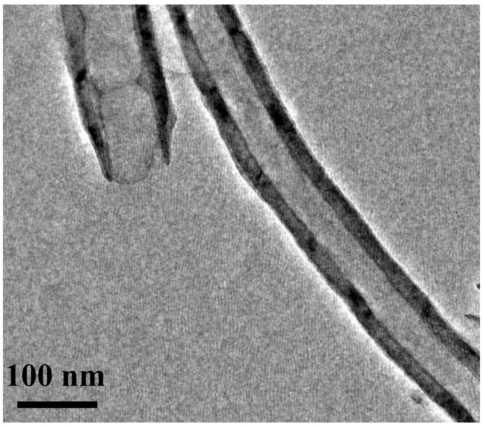

Fig. S3 Representative TEM image of the CNTs with a straight and open-ended channel.

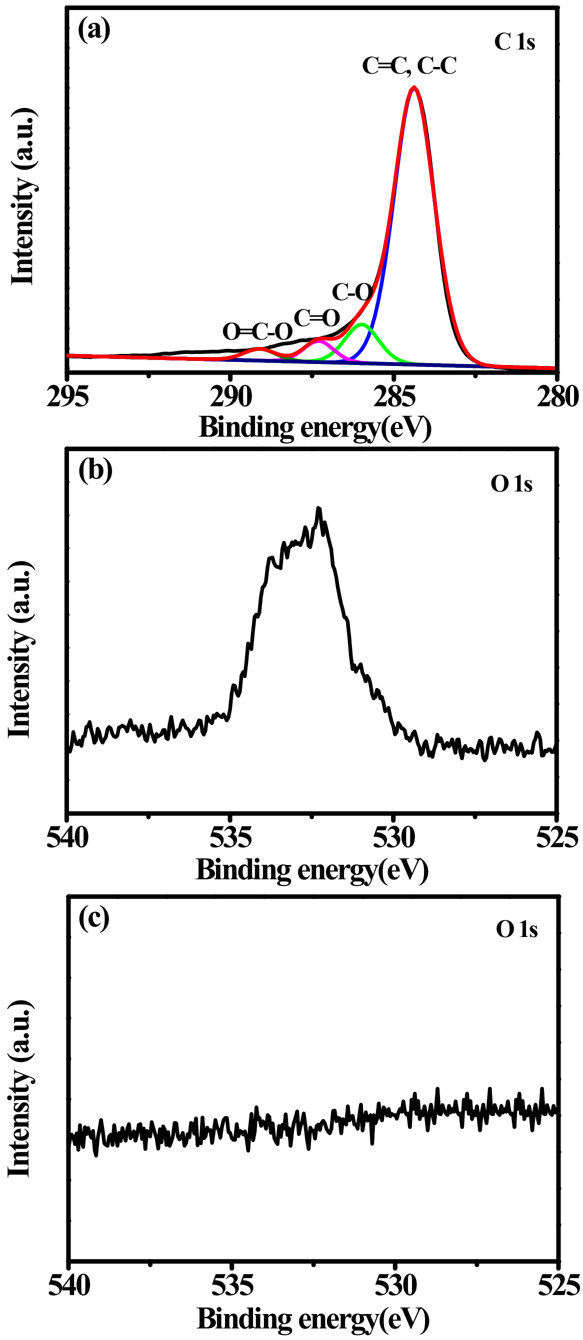

Fig. S4 High-resolution XPS spectra of (a) C1s and (b) O1s of CNTs. (c) Characteristic O 1s spectra of CNT after annealing at 800 ^{o}C.

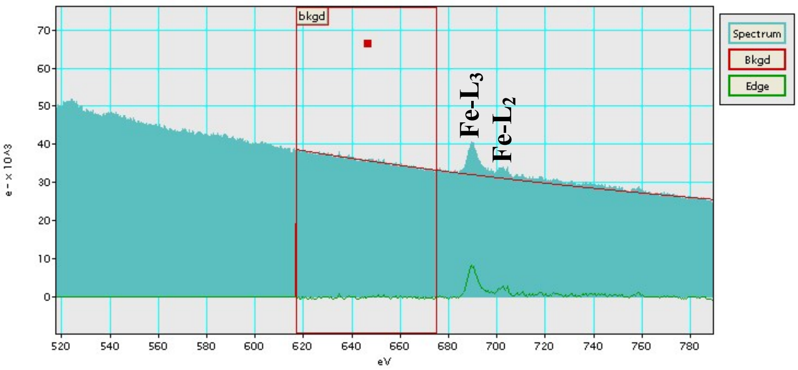

Fig. S5 EELS spectrum of Fe_3O_4@CNT

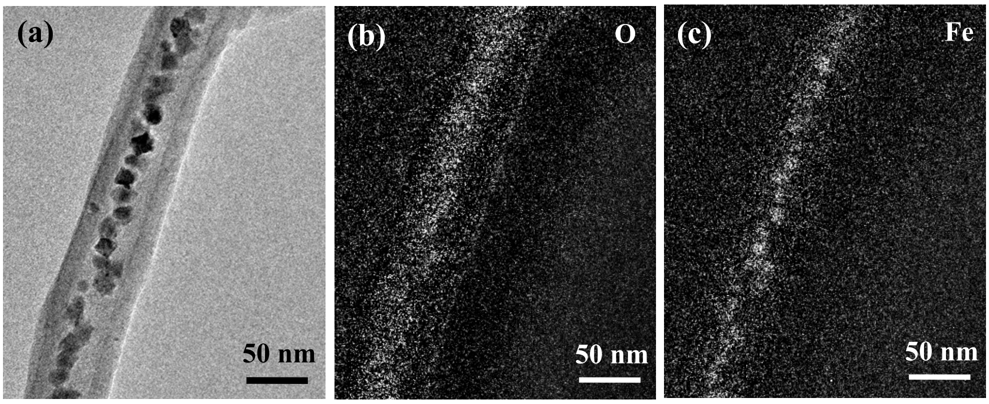

Fig. S6 TEM image of Fe_3O_4@CNT nanocomposite and corresponding element mappings of (b) O, (c) Fe

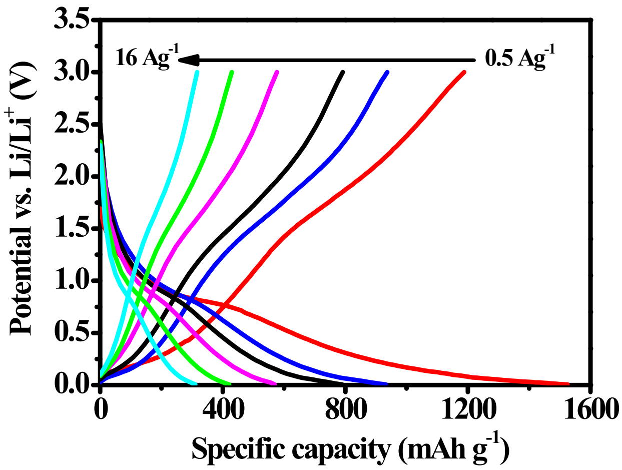

Fig. S7 Voltage profiles of the Fe_3O_4@CNT nanocomposite at different rates

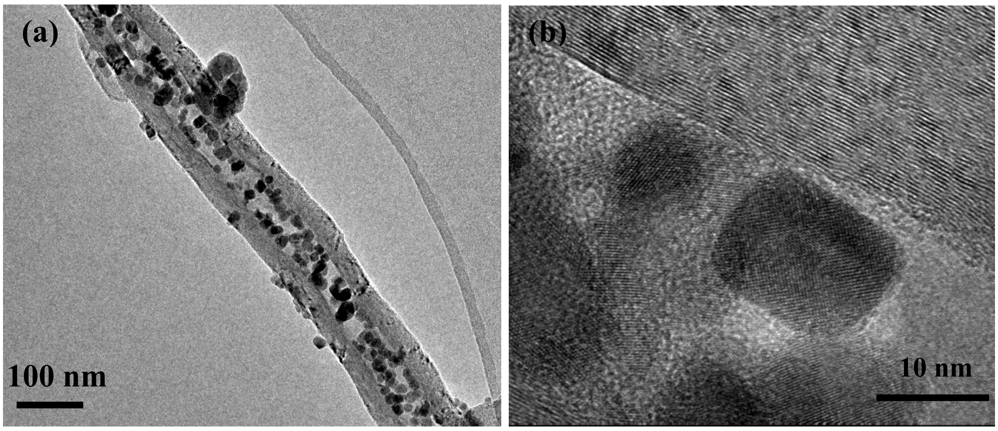

Fig. S8 TEM images of Fe_3O_4@CNT nanocomposite after 200th cycle at the current density of 1 A g^{-1}.

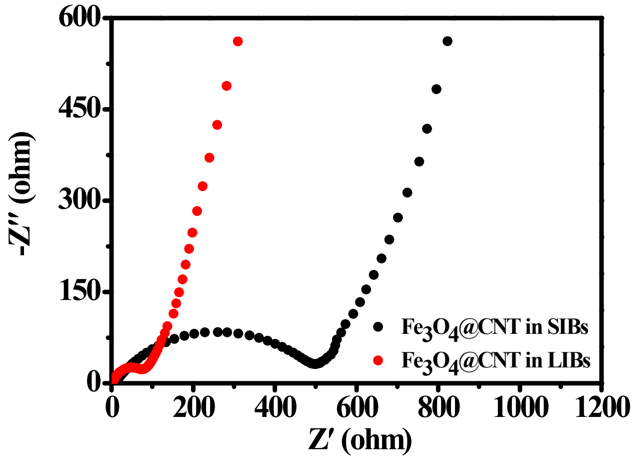

Fig. S9 The Nyquist plots of Fe_3O_4@CNT electrode in LIBs and SIBs

Table S1 Specific capacities of Fe_3O_4/CNT mixture, Fe_3O_4 nanoparticles, and CNTs at different current densities

Current density (A g^{-1})	Fe_3O_4/CNT (mAh g^{-1})	Fe_3O_4 (mAh g^{-1})	CNTs (mAh g^{-1})
0.5	660(10th)	578(10th)	270(10th)
1	530(20th)	368(20th)	187(20th)
2	426(30th)	248(30th)	132(30th)
4	285(40th)	166(40th)	101(40th)
8	189(50th)	91(50th)	74(50th)
16	142(60th)	60(60th)	56(60th)

Table S2 Lithium storage performance comparison of specific capacities of the Fe_3O_4@CNT nanocomposite with other Fe_3O_4-based materials reported in the literatures.

Fe_3O_4-based materials	Capacity (mAh g^{-1}) at different Current density	Ref.
Fe_3O_4@CNT nanocomposite	~923(100 cycles) at 0.5 A g^{-1} ~720(200 cycles) at 1 A g^{-1} ~615(200 cycles) at 2 A g^{-1}	This work
Hollow nitrogen (N)-doped Fe_3O_4/carbon nanocages	~700 (100 cycles) at 0.2 A g^{-1}	[51]
Graphene-Fe_3O_4@Carbon Nanocomposites	~710(50 cycles) at 0.1 A g^{-1}	[28]
Porous Fe_3O_4/C Microbelts	~710(50 cycles) at 0.1 A g^{-1}	[52]
Fe_3O_4/C Nanotubes	~600(100 cycles) at 0.15 C	[37]
Fe_3O_4@C Microcapsules	~600(50 cycles) at 0.928 A g^{-1}	[12]
Graphene-Encapsulated Hollow Fe_3O_4 Nanoparticle	~900 (50 cycles) at 0.1 A g^{-1}	[10]
Fe_3O_4/Fe/carbon	~600 (40 cycles) at 0.05 A g^{-1}	[53]
Fe_3O_4-graphene	~539 (200 cycles) at 1 A g^{-1}	[54]
Fe_3O_4-GNS	~650 (100 cycles) at 0.1 A g^{-1}	[55]
Fe_3O_4-graphene	~410 (75 cycles) at 1 A g^{-1}	[56]
Fe_3O_4@C@PGC	~792 (350 cycles) at 5 A g^{-1}	[13]
Carbon-coated Fe_3O_4 nanotube	~840 (300 cycles) at 1 A g^{-1}	[59]

Table S3 Comparison of specific capacities of the Fe_3O_4@CNT nanocomposite with other Fe_3O_4-based materials as anodes for SIBs.

Fe_3O_4-based materials	Capacity (mAh g^{-1}) at different Current density	Ref.
Fe_3O_4@CNT nanocomposite	~ 377(300 cycles) at 0.1 A g^{-1}	This work
C/Fe_3O_4/CNTs	~320 (50 cycles) at 0.05A g^{-1}	[50]
RGO/Fe_3O_4	~204(200 cycles) at 0.04 A g^{-1}	[57]
Fe_3O_4 nanoparticles	~160(30 cycles) at 0.02 A g^{-1}	[58]
Fe_3O_4 materials	~250(10 cycles) at 0.055A g^{-1}	[49]
Fe_3O_4 nanoparticles/graphene	~213(260 cycles) at 0.1A g^{-1}	[48]
Fe_3O_4 QD@C-GN	~343(1000 cycles) at 2A g^{-1}	[60]
Porous carbon-encapsulated Fe_3O_4	~450 (100 cycles) at 0.2A g^{-1}	[61]

[51] L.Wang, J. F. Wu, Y. Q. Chen, X. H. Wang, R. H. Zhou, S. H. Chen, Q. H. Guo, H. Q. Hou and Y. H. Song, Electrochimica Acta, 2015, 186, 50.

[52] L. M. Lang and Z. Xu, ACS Appl. Mater. Interfaces, 2013, 5, 1698.

[53] X. Y. Zhao, D. G. Xia and K. Zheng, ACS Appl. Mater. Interfaces, 2012, 4, 1350.

[54] Y. Dong, R. Ma, M. Hu, H. Cheng, Q. Yang, Y. Y. Li and J. A. Zapien, Phys. Chem. Chem. Phys, 2013, 15, 7174.

[55] J. Z. Wang, C. Zhong, D. Wexler, N. H. Idris, Z. X. Wang, L. Q. Chen and H. K.

Liu, Chem. Eur. J., 2011, 17, 661.

[56] P. C. Lian, X. F. Zhu, H. F. Xiang, Z. Li, W. S. Yang and H. H. Wang, Electrochim. Acta, 2010, 56, 834.

[57] S. H. Zhang, W. J. Li, B. Tan, S. L. Chou, Z. Li and S. X. Dou, J. Mater. Chem. A, 2015, 3, 4793.

[58] S. Komaba, T. Mikumo, N. Yabuuchi, A. Ogata, H. Yoshida and Y. Yamada, J. Electrochem. Soc., 2009, 157, A60.

[59] F. Han, L. J. Ma, Q. Sun, C. Lei and A. H. Lu, Nano Research, 2014, 7, 1706.

[60] L. Y. Qi, Y. W. Zhang, Z. C. Zuo, Y. L. Xin, C. K. Yang, B. Wu, X. X. Zhang and H. H. Zhou, J. Mater. Chem. A, 2016, 4, 8822.

[61] Y. P. Zhou, W. P. Sun, X. H. Rui, Y. Zhou, W. J. Ng, Q. Y. Yan and E. Fong, Nano Energy, 2016, 21, 71.